ACS Catalysis

Research Article

pubs.acs.org/acscatalysis

Glycerol Hydrogenolysis to Propylene Glycol and Ethylene Glycol on Zirconia Supported Noble Metal Catalysts

Shuai Wang, Kehua Yin, Yichi Zhang, and Haichao Liu*

Beijing National Laboratory for Molecular Sciences, State Key Laboratory for Structural Chemistry of Unstable and Stable Species, College of Chemistry and Molecular Engineering, Peking University, Beijing 100871, China

Supporting Information

ABSTRACT: Monoclinic zirconia (m-ZrO_2) supported Ru, Rh, Pt, and Pd nanoparticles with controlled sizes were prepared and examined in glycerol hydrogenolysis to propylene glycol and ethylene glycol at similar conversions in the kinetic regime. Their activity (normalized per exposed surface metal atom, i.e., turnover rate) and selectivity depend sensitively on the nature of the noble metals and their particle size. At a similar size (ca. 2 nm), Ru exhibited a greater turnover rate than Rh, Pt, and Pd, and the rate decreased in the sequence Ru ≫ Rh > Pt > Pd by a factor of about 25 (from 0.035 to 0.0014 mol glycerol (mol surface metal·s)$^{-1}$) at 473 K and 6.0 MPa H_2. Following such activity sequence, Ru was more prone to catalyze excessive cleavage of C−C bonds, leading to the formation of ethylene glycol and methane, while Pd exhibited the highest selectivity to cleavage of C−O bonds to propylene glycol. Similarly, larger Ru particles possessed higher glycerol hydrogenolysis activity concurrently with higher selectivities to ethylene glycol and especially methane at the expense of propylene glycol in the range of 1.8−4.5 nm. Analysis of kinetics and thermodynamics for the proposed elementary steps involving kinetically relevant glycerol dehydrogenation to glyceraldehyde leads to expressions of glycerol hydrogenolysis rate and selectivity to cleavage of C−O bonds relative to C−C bonds. Together with different effects of reaction temperature and atmosphere of H_2 and N_2 on the activity and selectivity for Ru/m-ZrO_2 and Pt/m-ZrO_2, these results suggest that the observed difference for different noble metals and particle sizes can be attributed to the difference in the strength of adsorption of glycerol and glyceraldehyde, derived from their different availability of unoccupied d orbitals.

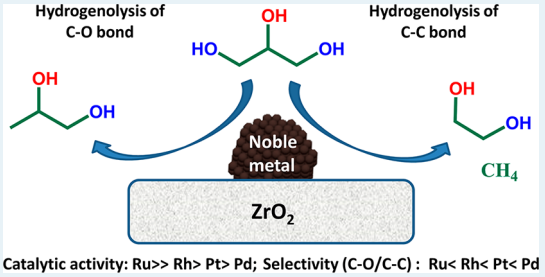

KEYWORDS: *glycerol, selective hydrogenolysis, propylene glycol, ethylene glycol, noble metal, size effect*

1. INTRODUCTION

Selective hydrogenolysis of glycerol to propylene glycol and ethylene glycol provides a viable route to utilize the large surplus of glycerol, the principal byproduct from the biodiesel production.[1] This reaction also provides an appropriate probe for studying the selective cleavage of C−O and C−C bonds in the catalytic hydrodeoxygenation of biomass-derived polyols,[2−4] which is regarded as an important process for future biorefineries.[5,6] As a consequence, glycerol hydrogenolysis has been intensively studied in the past decade,[1−3] and various metal-based catalysts have been accordingly explored, including Ru,[7−10] Rh,[11] Pt,[12] Pd,[13] Ir,[14] Ni,[15] Co,[16] Cu,[17−23] and Ag.[24] Specifically, the noble metals, that is, Ru, Rh, Pt, and Pd, have received great attention because of their superior catalytic activity[1,2] and hydrothermal stability[6] in glycerol hydrogenolysis.

Glycerol hydrogenolysis on the noble metals is structure sensitive, depending on their surface structure and particle size.[25] Montassier et al. primarily reported that the turnover rate per surface Ru atom on Ru/C increased sharply with the Ru particle size in the range of 1.2−4.2 nm, while the selectivities to propylene glycol and ethylene glycol changed slightly at 483 K and 6 MPa.[26] However, Wang et al. found that the turnover rate of the Ru particles supported on multiwalled carbon nanotubes decreased by two-thirds when the particle size increased from 3 to 10 nm, whereas the selectivities to propylene glycol and ethylene glycol increased significantly (from 32% to 58% and 10% to 21%, respectively) at 473 K and 4.0 MPa H_2.[27] Different from such inconsistent size effects, Ru generally exhibits higher activity, but also higher selectivity to cleavage of C−C bonds over C−O bonds than Rh, Pt, and Pd in glycerol hydrogenolysis especially under neutral conditions.[28] For instance, Maris and Davis found that the turnover rate of Ru on active carbon was about 2-fold greater than that of Pt with the same metal particle size of 2.3 nm at 473 K and 4.0 MPa H_2, while the selectivity ratios of propylene glycol to ethylene glycol on Ru/C and Pt/C were 0.5 and 4.6, respectively.[8] Recently, van Ryneveld et al. also reported a hydrogenolysis activity order of Ru/Al_2O_3 > Pd/Al_2O_3 > Pt/Al_2O_3 with 1 nm metal particles at 453 K and 8.0 MPa H_2, and the corresponding cleavage ratios of C−O/C−C bonds showed an opposite trend.[29]

To improve the activity and selectivity on the noble metal catalysts, recent studies have focused on the promoting effects

Received: June 28, 2013
Revised: July 30, 2013
Published: August 1, 2013

Table 1. Metal Particle Sizes, Turnover Rates, and Selectivities in Glycerol Hydrogenolysis for m-ZrO_2-Supported Ru, Rh, Pt, and Pd and γ-Al_2O_3 Supported Ru with 2 wt % Metal Loading[a]

				selectivity[c] (%)				
catalyst	d_{H_2}[b] (nm)	conversion (%)	turnover rate[e]	propylene glycol	ethylene glycol	CH_4	ethanol	propanol[d]
Ru/m-ZrO_2	2.3	22.9	34.9	45.7	21.0	25.0	5.4	2.9
Ru/γ-Al_2O_3	2.1	18.7	22.1	14.3	34.5	44.3	3.7	3.2
Rh/m-ZrO_2	2.2	22.8	9.1	65.6	12.4	15.7	3.8	2.5
Pt/m-ZrO_2	2.4	20.4	5.6	85.7	7.4	trace	0.8	6.1
Pd/m-ZrO_2	2.1	21.0	1.4	90.5	5.5	trace	0.5	3.5

[a]Reaction conditions: 50 cm^3 10 wt % glycerol aqueous solution, 473 K, 6.0 MPa H_2, 3 h, about 20% glycerol conversion obtained by varying the catalyst amount. [b]Metal particle sizes measured by H_2-chemisorption. [c]Trace amounts of CO_2 and methanol were detected in the products and not shown here. [d]Including 1-propanol and 2-propanol. [e]10^{-3} mol glycerol (mol surface metal·s)$^{-1}$.

of second metal components and acid-basic functions in glycerol hydrogenolysis.[3,28] Addition of non-noble metal such as Cu and Fe into Ru concurrently improved the C−O cleavage to propylene glycol and suppressed the C−C cleavage to ethylene glycol.[10,30] Such effects were also observed for Pd−Fe, Pd−Zn, and Pd−Ni bimetallic catalysts.[31] Tomishige and co-workers increased the glycerol hydrogenolysis rate by about three fold and the propylene glycerol selectivity from 26% to 55% by mixing an acidic ion-exchange resin with Ru/C.[32] Alhanash et al. obtained about 96% propylene glycerol selectivity at 21% glycerol conversion at 423 K and 0.5 MPa H_2 on an acidic $Cs_{2.5}H_{0.5}[PW_{12}O_{40}]$-supported Ru catalyst, although the selectivity decreased to 88% when the conversion increased to 31%.[33] Yuan et al. found that the activity of glycerol hydrogenolysis and selectivity to propylene glycol on Pt-based catalysts increased with their support basicity.[12] Feng et al. reported that addition of LiOH significantly improved the propylene glycol selectivity from 48% to 87% with the concurrent increase in the glycerol conversion from 66% to 90% on Ru/TiO_2 at 443 K and 3 MPa H_2.[9] Noticeably, acid sites on sulfated zirconia, WO_3, and ReO_x can cooperate with the noble metals such as Pt and Ir, leading to selective hydrogenolysis of the secondary hydroxyl group of glycerol to form 1,3-propanediol.[14,34,35] For example, a high 1,3-propanediol yield of about 56% was achieved on Pt/sulfated ZrO_2 at 443 K and 7.3 MPa H_2.[34] Clearly, these previous efforts and advances have provided a basis for further improving the efficiency of the noble metals, which will be beneficial to this study toward a fundamental understanding that is still unclear on the intrinsic catalytic activity and selectivity of the noble metals and effects of their particle size in glycerol hydrogenolysis.

In this work, we prepare supported Ru, Rh, Pt, and Pd catalysts with similar metal dispersions on hydrothermally stable monoclinic ZrO_2 (m-ZrO_2), and compare their intrinsic activities and selectivities in glycerol hydrogenolysis at similar glycerol conversions within the kinetic regime. We also examine the effects of reaction temperature, atmosphere (H_2 and N_2), and metal particle size, in attempts to unveil the reaction mechanism of glycerol hydrogenolysis and the factors dictating the cleavage of C−C and C−O bonds on the noble metal catalysts.

2. EXPERIMENTAL SECTION

2.1. Preparation of Catalysts. Pure m-ZrO_2 was synthesized using a facile hydrothermal method reported previously.[36] Certain amounts of zirconyl nitrate ($ZrO(NO_3)_2·2H_2O$, A.R., Beijing Chemical) and urea ($CO(NH_2)_2$, A.R., Beijing Chemical) were dissolved in 80 cm^3 deionized water with a Zr^{4+} concentration of 4.0×10^{-4} mol cm^{-3} and a urea/Zr^{4+} molar ratio of 10/1. The solution was then placed in a Teflon-lined stainless-steel autoclave (100 cm^3) and held at 433 K under autogenous pressure for 20 h. Afterward, the resulting precipitates were washed with deionized water until the filtrates were neutral and then treated subsequently in ambient air at 383 K overnight and at 673 K for 4 h. The as-synthesized m-ZrO_2 support was measured to have a Brunauer−Emmett−Teller (BET) surface area of 131 m^2/g.

Ru, Rh, Pt, and Pd nanoparticles supported on m-ZrO_2 were prepared by incipient wetness impregnation, including Ru/m-ZrO_2 with Ru loadings of 0.51, 1.0, 2.1, 2.9, 4.0, and 4.8 wt %, 2.0 wt % Rh/m-ZrO_2, 2.0 wt % Pt/m-ZrO_2, and 2.1 wt % Pd/m-ZrO_2. $RuCl_3·nH_2O$ (G.R., Sinopharm Chemical), $RhCl_3·nH_2O$ (A.R., Alfa Aesar), $H_2PtCl_6·6H_2O$ (A.R., Beijing Chemical), and $PdCl_2$ (A.R., Shenyang Research Institute of Nonferrous Metals) were used as the metal precursors dissolved in deionized water. After impregnation, these catalysts were treated at 383 K overnight in dry air, and then reduced in flowing 20% H_2/N_2 (>99.99%, Beijing Huayuan) by heating to 673 K at a ramping rate of 0.083 K s^{-1} and holding at 673 K for 3 h. Similarly, 2.2 wt % Ru/γ-Al_2O_3 was also prepared, and a commercial γ-Al_2O_3 (A.R., Alfa Aesar) with a BET surface area of 195 m^2/g was used as the support.

2.2. Catalyst Characterization. Crystalline structures of the catalysts were characterized by X-ray diffraction (XRD) on a Rigaku D/MAX-2400 diffractometer using Cu $K_{\alpha 1}$ radiation (λ = 1.5406 Å) operated at 40 kV and 100 mA. The noble metal particle sizes of the catalysts were measured by transmission electron microscopy (TEM) and H_2-chemisorption. TEM images of fresh samples were obtained at an acceleration voltage of 300 kV on Philips Tecnai F30 FEGTEM. H_2-chemisorption for the supported Ru, Rh, and Pt samples was performed at 313 K and 10−50 kPa H_2 using a Quantachrome Autosorb-1 analyzer after the samples were treated in flowing 5% H_2/N_2 (>99.99%, Beijing Huayuan) at 623 K for 2 h and then evacuated at the same temperature for 12 h.[37] For 2 wt % Pd/m-ZrO_2, H_2-chemisorption was performed at 343 K and 0.4−1.5 kPa H_2 to avoid the formation of the β hydride phase. Metal particle sizes for the samples were accordingly calculated from the H_2-chemisorption results by assuming the chemisorption stoichiometry of H/metal molar ratio of 1.0 and that the metal particles were spherical.

2.3. Catalytic Reaction. Glycerol hydrogenolysis reactions were carried out in a Teflon-lined stainless steel autoclave (100 mL) at a stirring speed of 800 rpm. In a typical run, 50 g of 10 wt % glycerol (A.R., Beijing Chemical) aqueous solution and 0.35 g of metal catalyst were placed in the autoclave. After fully

dx.doi.org/10.1021/cs400486z | ACS Catal. 2013, 3, 2112−2121

purging the autoclave with H_2 (>99.99%, Beijing Huayuan), the reactor was pressurized with H_2 to 6.0 MPa and then heated to the reaction temperatures (453−513 K). Liquid products were separated by centrifugation and analyzed by gas chromatography (Agilent 7890A GC) using a capillary column (AT-Aquawax: 30 m × 0.25 mm × 0.25 m) connected to a flame ionization detector. 1-Butanol and 1,4-butanediol were used as external standards for volatile products (e.g., methanol, ethanol, 1-propanol, and acetal) and products of high boiling points (e.g., ethylene glycol, propylene glycol, and glycerol), respectively. Gas products, mainly methane and CO_2, were analyzed by gas chromatography (Shimadzu 2010 GC, Porapak-Q column) with a thermal conductivity detector. The carbon balance of the analysis was generally within 100 ± 5%. Reaction activities were reported by the molar glycerol conversion rates per mole of exposed metal atoms (estimated from the H_2-chemisorption data described above), that is, turnover rates (mol glycerol (mol surface metal·s)$^{-1}$) and product selectivities were reported on the carbon basis, as employed by Miyazawa et al.[7]

3. RESULTS AND DISCUSSION

3.1. Activity and Selectivity of Supported Noble-Metal Catalysts in Glycerol Hydrogenolysis. Table 1 shows glycerol hydrogenolysis activities and selectivities on Ru/m-ZrO_2, Rh/m-ZrO_2, Pt/m-ZrO_2, and Pd/m-ZrO_2, and also for comparison on Ru/γ-Al_2O_3 with 2 wt % metal loading at 473 K and 6.0 MPa H_2. The five catalysts present merely the XRD patterns of the corresponding support of m-ZrO_2 or γ-Al_2O_3 (Figure 1). The absence of the characteristic diffraction peaks

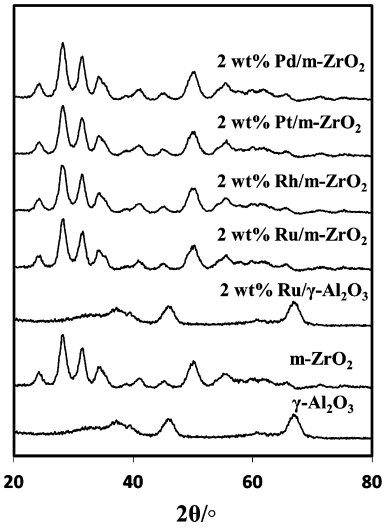

Figure 1. X-ray diffraction patterns for m-ZrO_2-supported Ru, Rh, Pt, and Pd with 2 wt % metal loading, γ-Al_2O_3-supported Ru with 2 wt % metal loading, and the corresponding supports of m-ZrO_2 and γ-Al2O_3 as references.

of the noble metals indicates that the metals were highly dispersed on the supports. TEM and H_2-chemisorption characterization results confirm the XRD results, showing that the metal particles of these catalysts possessed similar average sizes (~2 nm) and narrow size distributions, irrespective of the identity of the metal and support (Figure 2 and Table 1). Such catalyst properties enable us to compare their intrinsic activity and selectivity in glycerol hydrogenolysis, free of the known effects of the metal particle size prevalently found for many reactions.

The glycerol hydrogenolysis activities in Table 1 were normalized by the number of exposed metal atoms estimated from the results of H_2-chemisorption, which represent the turnover rates and reflect the intrinsic activity of the accessible metal atoms. Detected products included propylene glycol, 1-propanol, and 2-propanol, which were formed via cleavage of C−O bonds of glycerol, and ethylene glycol, ethanol, methanol, methane, and CO_2, which were formed via cleavage of C−C bonds, as reported previously.[7] The turnover rates and selectivities were compared at similar glycerol conversions of approximately 20% within the kinetic regime. As shown in Table 1, Ru/m-ZrO_2 showed a higher turnover rate than Ru/γ-Al_2O_3 with a similar Ru particle size of 2 nm (0.035 vs 0.022 mol glycerol (mol surface Ru·s)$^{-1}$). Selectivities to propylene glycol, ethylene glycol, and methane on Ru/m-ZrO_2 were 45.7%, 21.0%, and 25.0%, respectively, at ~20% glycerol conversion. On Ru/γ-Al_2O_3, the selectivity to propylene glycol decreased to 14.3%, whereas the selectivity to ethylene glycol increased to 34.5% with a large amount of methane (44.3% selectivity). Such difference in the hydrogenolysis activity and selectivity between the two Ru catalysts is clearly not due to the difference in their metal particle sizes, but due to the strong support effect. It is known that m-ZrO_2 surface possesses stronger basicity than γ-Al_2O_3,[38] facilitating the kinetically relevant cleavage of the α-C-H bond of glycerol, and the selective formation of propylene glycol on the Ru surface, as discussed below.

Glycerol hydrogenolysis is sensitive to the property of the noble metals as well. Compared with Ru/m-ZrO_2, the turnover rates on Rh/m-ZrO_2, Pt/m-ZrO_2, and Pd/m-ZrO_2 decreased from 0.035 to 0.0091, 0.0056, and 0.0014 mol glycerol (mol surface metal·s)$^{-1}$, respectively (Table 1). Specifically, the catalytic activity of Ru/m-ZrO_2 was about 25 times greater than that of Pd/m-ZrO_2. The selectivities to the products via the cleavage of C−O and C−C bonds presented the opposite trends with the variation of the noble metals (Table 1). At ~20% glycerol conversion, Ru/m-ZrO_2 exhibited the lowest selectivity to propylene glycol (45.7%), and the highest selectivities to ethylene glycol (21.0%) and methane (25.0%) among the four m-ZrO_2 supported noble metal catalysts. The selectivity to propylene glycol increased to 65.6%, and the selectivities to ethylene glycol and methane decreased to 12.4% and 15.7%, respectively, on Rh/m-ZrO_2. On Pd/m-ZrO_2, the selectivity to propylene glycol was as high as 90.5% while the selectivities to ethylene glycol decreased to 5.5% with the negligible formation of methane. Such strong effects of the noble metals, as discussed below, are closely relevant to their effects on the reaction pathways of glycerol hydrogenolysis.

Two reaction routes, that is, dehydration and dehydrogenation routes, for glycerol hydrogenolysis to propylene glycol have been intensively discussed in the literature.[2,3] In the dehydration route, glycerol directly dehydrates to acetol on acid sites, which then hydrogenates to propylene glycol on metal sites.[7] In the dehydrogenation route, glycerol first dehydrogenates to glyceraldehyde on metal sites, followed by its dehydration and subsequent hydrogenation to acetol and propylene glycol.[8] Our control experiments showed that pure m-ZrO_2 and γ-Al_2O_3 did not give detectable glycerol conversion in the absence of the noble metals under the identical conditions used in this study, suggesting that the metal sites are prerequisite for the initial activation and reaction of

dx.doi.org/10.1021/cs400486z | ACS Catal. 2013, 3, 2112−2121

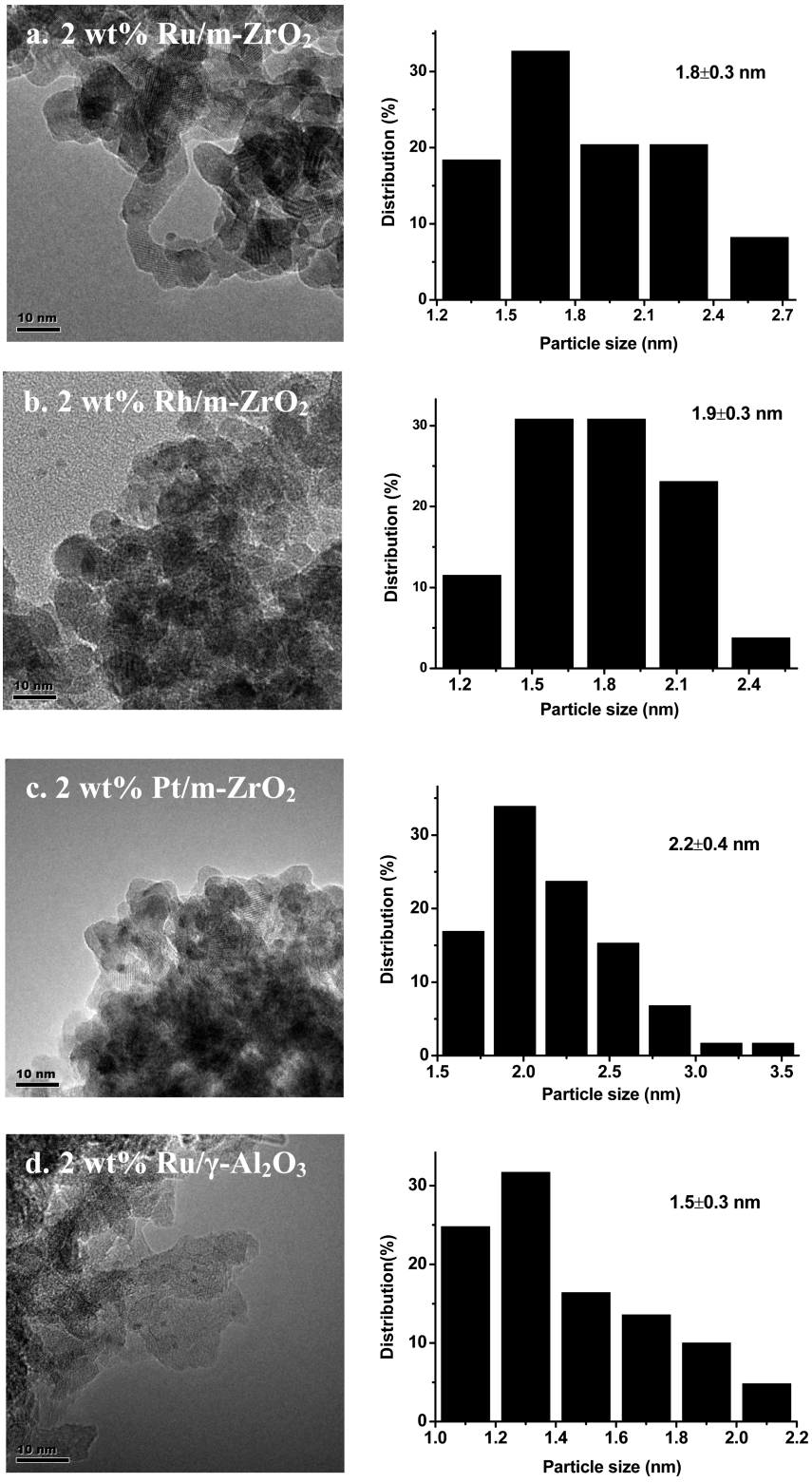

Figure 2. Transmission electron microscopy micrographs and histograms of metal particle size distribution for m-ZrO_2-supported Ru, Rh, and Pt and γ-Al_2O_3-supported Ru with 2 wt % metal loading (scale bar = 10 nm). (a) 2 wt % Ru/m-ZrO_2, (b) 2 wt % Rh/m-ZrO_2, (c) 2 wt % Pt/m-ZrO_2, and (d) 2 wt % Ru/γ-Al_2O_3.

glycerol. Such inertness of the two oxide supports for glycerol hydrogenolysis were also observed by Vasiliadou et al., who proposed that metal sites correlated with the dehydration rate of glycerol.[39] Recently, Anueau et al. reported that the dehydrogenation route is kinetically more favorable than the dehydration route on a Rh surface based on their experimental and theoretical results.[11] Consistent with this study, glyceraldehyde from the dehydrogenation of glycerol has also been proposed as an intermediate for ethylene glycol via its C−C bond cleavage and for C_1 products via its decarbonylation on

dx.doi.org/10.1021/cs400486z | ACS Catal. 2013, 3, 2112−2121

Scheme 1. Proposed Pathways for Cleavage of C−O and C−C Bonds in Glycerol Hydrogenolysis on Noble Metal Catalysts

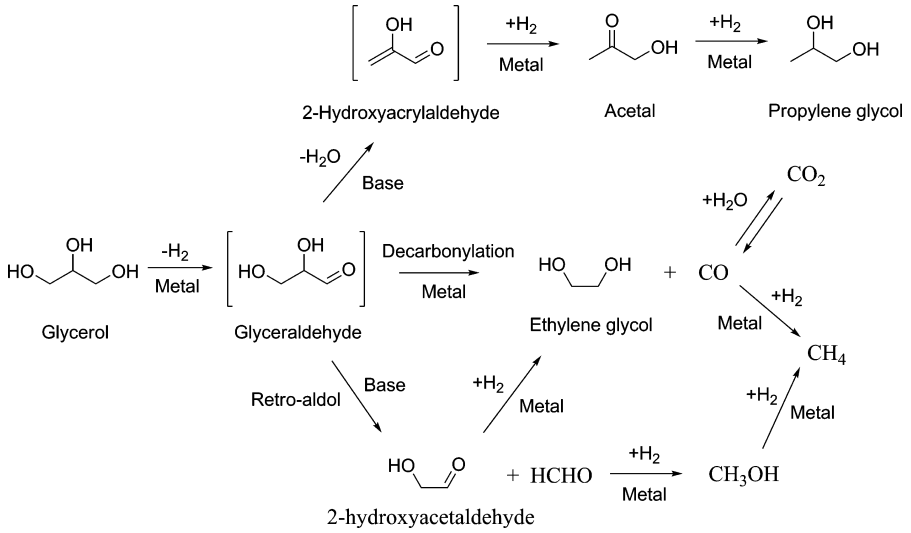

noble metal surfaces[40] or via retro-aldol condensation on basic sites.[41] Therefore, we assume that the dehydrogenation route is dominant in glycerol hydrogenolysis on the supported noble metal catalysts in our reaction conditions.

Together with the studies in the literature,[8,40,42] the reaction pathways of glycerol hydrogenolysis are proposed in Scheme 1. Glycerol dehydrogenates to glyceraldehyde on the noble metal surface. Then the glyceraldehyde intermediate undergoes dehydration to form 2-hydroxyacrylaldehyde, which hydrogenates sequentially to acetol and propylene glycol. Alternatively, glyceraldehyde converts to ethylene glycerol and CO via its decarbonylation on the noble metal surfaces or to the 2-hydroxyacetaldehyde and formaldehyde intermediates via retro-aldol condensation on the basic sites, which further hydrogenate to ethylene glycol and methanol, respectively. The formation of methane is mainly contributed from hydrogenolysis of methanol and hydrogenation of CO on noble metals.[42] Moreover, CO may convert to CO_2 via water gas shift reaction. Such proposed reaction pathways on the noble metals are similar to those on Cu-based catalysts,[18] except for the insignificant cleavage of the C−C bonds because of the known low catalytic activity of the Cu surface for the decarbonylation reaction. Instead, glyceraldehyde tends to degrade through the retro-Claisen route to form ethylene glycol on the Cu surface.[18] In addition, the primary hydrogenolysis products, propylene glycerol and ethylene glycerol, undergo further hydrogenolysis reactions to form 1-propanol and ethanol, and so on (not shown in Scheme 1 for clarity).

The undetectable amount of glyceraldehyde in the liquid products indicates that dehydrogenation of glycerol to glyceraldehyde on the metal surfaces was irreversible and far from the equilibrium. Consistently, the dehydrogenation step has been suggested to be kinetically relevant to the glycerol hydrogenolysis in neutral and basic conditions as evidenced both on noble metals[8,11] and Cu-based catalysts.[18,19] According to the reaction pathways discussed above, the reaction rates of glycerol hydrogenolysis (r_{Gly}) are determined by the step of glycerol dehydrogenation to glyceraldehyde on metal surfaces, while the rate ratios of the primary hydrogenolysis of C−O bonds (leading to the formation of propylene glycol) and C−C bonds (leading to the formation of ethylene glycol and the C_1 products, etc.), denoted as r_{C-O}/r_{C-C}, are determined by the relative rates of glyceraldehyde dehydration to direct decarbonylation and retro-aldol condensation of glyceraldehyde (Scheme 1). The turnover rates on Ru/m-ZrO_2, Rh/m-ZrO_2, Pt/m-ZrO_2, and Pd/m-ZrO_2 at similar metal dispersions and kinetic regimes indicate that the intrinsic dehydrogenation ability of noble metals follows the sequence Ru ≫ Rh > Pt > Pd, which is consistent with the results for 2-propanol dehydrogenation on the noble metals reported by Ukisu and Miyadera.[43] Specifically, they suggested the cleavage of α-C-H bond of glycerol in its dehydrogenation step is kinetically relevant.[43] Maris and Davis have demonstrated that both dehydration and retro-aldol condensation of the glyceraldehyde intermediate are base-catalyzed reactions in glycerol hydrogenolysis.[8] Accordingly, the observed variation of the ethylene glycol selectivity with the noble metals on m-ZrO_2 (Table 1) indicates that the C−C bond cleavage in glycerol hydrogenolysis mostly occurs via glyceraldehyde decarbonylation on the metal surfaces rather than via retro-aldol condensation. Otherwise, the selectivities to the aforementioned products via cleavage of C−O and C−C bonds should be determined by the basicity of the m-ZrO_2 support, irrespective of the identity of the noble metals.

Scheme 2 lists a proposed sequence of elementary steps, which are related to r_{Gly} and r_{C-O}/r_{C-C}, and the associated kinetic and thermodynamic constants. Here r_{Gly} and r_{C-O}/r_{C-C}

Scheme 2. . Proposed Sequence of Elementary Steps and Associated Kinetic or Thermodynamic Constants in Glycerol Hydrogenolysis Catalyzed by Noble Metals

1. Glycerol adsorption	$C_3H_8O_3 + * \rightleftharpoons C_3H_8O_3*$	K_{Gly}
2. Alkoxide formation	$C_3H_8O_3* + * \rightleftharpoons C_3H_7O_3* + H*$	$K_{Alkoxide}$
3. Cleavage of α-C-H bond	$C_3H_7O_3* + * \longrightarrow C_3H_6O_3* + H*$	k_{DH}
4. Glyceraldehyde desorption	$C_3H_6O_3* \rightleftharpoons C_3H_6O_3 + *$	$1/K_{GA}$
5. H_2 desorption	$H* + H* \rightleftharpoons H_2 + 2*$	$1/K_{H2}$
6. Glyceraldehyde dehydration	$C_3H_6O_3 \longrightarrow C_3H_4O_2 + H_2O$	k_{DOH}
7. Decarbonylation	$C_3H_6O_3* + * \longrightarrow C_2H_6O_2* + CO*$	$k_{C=O}$
... ...		

dx.doi.org/10.1021/cs400486z | ACS Catal. 2013, 3, 2112−2121

are expressed as eqs 1 and 2 by applying the quasi-equilibrium assumption for Steps 1, 2, 4, and 5, in which k_{DH} and $k_{C=O}$ are the respective kinetic constants for the cleavage of the α-C-H bond of glycerol and glyceraldehyde decarbonylation on metal surfaces; k_{DOH} is the kinetic constant for glyceraldehyde dehydration catalyzed by basic sites on m-ZrO_2 in liquid phase; K_{Gly}, K_{GA}, and K_{H2} are the respective adsorption constants for glycerol, glyceraldehyde, and H_2, and $K_{Alkoxide}$ is the dissociation constant of glycerol to the alkoxide species on metal surfaces; c_{Gly} represents the molar concentration of glycerol in liquid phase; and θ_* refers to the concentration of vacant sites on metal surfaces. The details of the derivation of eqs 1 and 2 are included in the Supporting Information.

$$r_{Gly} = \frac{k_{DH}K_{Gly}K_{Alkoxide}}{K_{H2}^{1/2}}\frac{c_{Gly}}{P_{H_2}^{1/2}}\theta_*^2 \quad (1)$$

$$\frac{r_{C-O}}{r_{C-C}} = \frac{k_{DOH}}{k_{C=O}K_{GA}}\frac{1}{\theta_*^2} \quad (2)$$

Based on transition-state theory (eq 3) and the relationship between the equilibrium constant, enthalpy, and entropy of a reaction (eq 4), eq 2 is converted to its thermodynamic form, eq 5, in which $E_{a,DOH}$ and $E_{a,C=O}$ are the activation energies for glyceraldehyde dehydration and decarbonylation, respectively; $\Delta S^{\ddagger}_{DOH}$ and $\Delta S^{\ddagger}_{C=O}$ are the entropy changes from the reactant to the transition state for glyceraldehyde dehydration and decarbonylation, respectively; ΔH_{GA} and ΔS_{GA} are the adsorption enthalpy and entropy for glyceraldehyde on metal surfaces. It is clear from eqs 1 and 5 that r_{Gly} and r_{C-O}/r_{C-C} are both functions of the available vacant sites on metal surfaces. Therefore, varying the vacancy concentration of the metal surfaces, for example, by changing the reaction temperature or hydrogenolysis atmosphere from H_2 to N_2, can provide insight into the difference of the catalytic activity and selectivity among the different noble metals examined in this work, as shown in the next section.

$$k(T) = \frac{k_B T}{h}e^{(\Delta S^{\ddagger}+1)/R}e^{-E_a/RT} \quad (3)$$

$$K(T) = e^{\Delta S/R}e^{-\Delta H/RT} \quad (4)$$

$$\frac{r_{C-O}}{r_{C-C}} = \exp[(\Delta S^{\ddagger}_{DOH} - \Delta S^{\ddagger}_{C=O} - \Delta S_{GA})/R]\exp[-(E_{a,DOH} - E_{a,C=O} - \Delta H_{GA})/RT]\frac{1}{\theta_*^2} \quad (5)$$

3.2. Effects of Reaction Temperature and Atmosphere on Glycerol Hydrogenolysis. Figure 3 shows the turnover rates and selectivities for glycerol hydrogenolysis as a function of reaction temperature on the two representative catalysts, 2 wt % Ru/m-ZrO_2 and 2 wt % Pt/m-ZrO_2. The turnover rate of Ru/m-ZrO_2 increased exponentially from 0.019 to 0.133 mol glycerol (mol surface Ru·s)$^{-1}$ with increasing reaction temperature from 453 to 513 K, while the turnover rate of Pt/m-ZrO_2 increased from 0.0026 to 0.0082 mol glycerol (mol surface Pt·s)$^{-1}$ in the temperature range of 453−483 K. The calculated apparent activation energies for Ru/m-ZrO_2 and Pt/m-ZrO_2 from Figure 3 were 72 and 84 kJ/mol, respectively, which are consistent with the above statement that the alkanol dehydrogenation ability of Ru is superior to that of Pt.

The selectivity to propylene glycol on Ru/m-ZrO_2 increased from 47.2% to 56.5% at ~20% glycerol conversion when

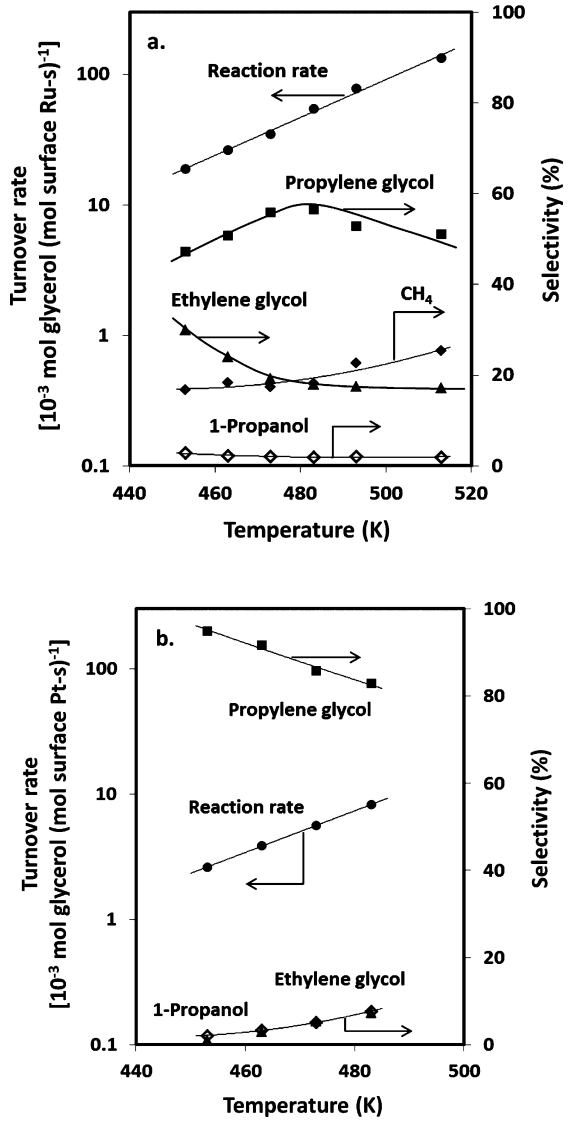

Figure 3. Effects of reaction temperature on turnover rates and selectivities for glycerol hydrogenolysis on Ru/m-ZrO_2 (a) and Pt/m-ZrO_2 (b) with 2 wt % metal loading. Reaction conditions: 50 cm^3 10 wt % glycerol aqueous solution, 6.0 MPa H_2, 3 h, about 20% glycerol conversion obtained by varying the catalyst amount.

increasing the reaction temperature from 453 to 483 K, and then decreased to 51.1% when the temperature further increased to 513 K (Figure 3a). The selectivities to ethylene glycol via C−C cleavage and 1-propanol via hydrogenolysis of propylene glycol decreased from 30.0% to 17.2% and from 2.8% to 1.9%, respectively, with increasing reaction temperature in the whole range of 453−513 K. Accompanying the above changes, the selectivity to methane increased monotonically from 16.8% to 25.3% with the reaction temperature (453−513 K). It is obvious that high temperatures favor the deep hydrogenolysis of glycerol to methane. Miyazawa et al. has reported that propylene glycol and 1-propanol are less reactive than ethylene glycol in hydrogenolysis reactions,[7] indicating that methane is mainly formed from the C−C cleavage of glycerol or further hydrogenolysis of ethylene glycol, but not from propylene glycol or 1-propanol. Noticeably, the total selectivities to propylene glycol, 1-propanol, ethylene glycol, and methane were always kept above 95% in this work. Such

dx.doi.org/10.1021/cs400486z | ACS Catal. 2013, 3, 2112−2121

excellent carbon balance enables us to compare the primary hydrogenolysis selectivities to the cleavage of C−O and C−C bonds by the selectivity ratios of the sum of propylene glycol and 1-propanol to the sum of ethylene glycol and methane. It is readily seen that the ratios of the primary hydrogenolysis selectivity of C−O bonds to that of the C−C bonds on Ru/m-ZrO_2 possessed a similar volcano-type dependence on the reaction temperature, and reached the maximum value at 483 K (Figure 4), as observed for the propylene glycol selectivity

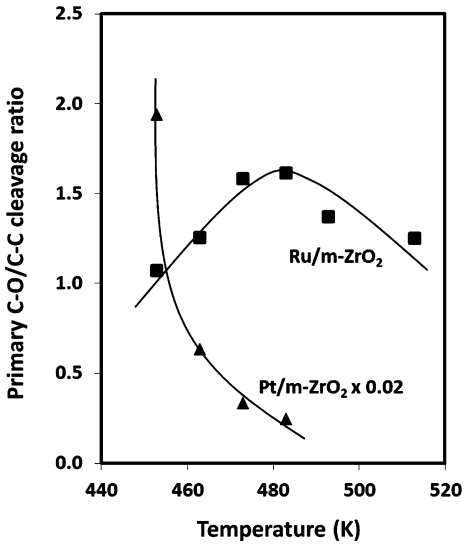

Figure 4. Primary C−O/C−C cleavage ratio for glycerol hydrogenolysis on Ru/m-ZrO_2 and Pt/m-ZrO_2 with 2 wt % metal loading. Reaction conditions: 50 cm^3 10 wt % glycerol aqueous solution, 6.0 MPa H_2, 3 h, ∼20% glycerol conversion obtained by varying the catalyst amount.

(Figure 3a). Different temperature effects on the selectivities were found for Pt/m-ZrO_2 (Figure 3b). No methane was formed in the reaction temperature range 453−513 K at about 20% glycerol conversion. The selectivity to propylene glycol monotonically decreased from 94.9% to 82.8% with concurrent increase in the selectivities to ethylene glycol and 1-propanol from 1.0% to 7.4% and 2.1% to 7.7%, respectively, as the temperature ramped from 453 to 513 K. Therefore, the primary C−O/C−C cleavage ratio on Pt/m-ZrO_2 decreased with increasing reaction temperature (Figure 4). Taken together, these results show that an increase of reaction temperature can improve the selective hydrogenolysis of C−O bonds in glycerol to propylene glycol on Ru/m-ZrO_2, but not on Pt/m-ZrO_2.

The dependence of the selectivity to the cleavage of C−O and C−C bonds is derived from eq 5. It is known that enthalpy and entropy apparently do not change with temperature. Therefore, the first term of eq 5 which has the contribution of entropy is nearly independent of the reaction temperature, whereas the third term $(1/\theta_*^2)$ decreases with the reaction temperature because the adsorption of glycerol and hydrogenolysis products on metal surfaces is exothermic ($\Delta H_{adsorption} < 0$). Thus, the source of the observed difference between Ru/m-ZrO_2 and Pt/m-ZrO_2 as it concerns the temperature effect on r_{C-O}/r_{C-C} lies in the second term of eq 5. Glyceraldehyde dehydration appears to occur readily, considering the thermodynamically favored formation of the π-conjugated dehydration product (2-hydroxyacrylaldehyde).[18] Moreover, the dehydration reaction is catalyzed by the basic sites on the m-ZrO_2 support, which means $E_{a,DOH}$ should be constant for all the m-ZrO_2-supported noble metal catalysts. In contrast, decarbonylation of carbonyl compounds on the noble metal surfaces involves a cleavage of C−C bonds and usually occurs at high temperature because of its large activation barrier.[44] Wang et al. reported that the cleavage of C−C bonds on the noble metals showed similar activation barriers.[45] For instance, the activation barriers for the conversion of CH_3CH_2* surface species to CH_3* and CH_2* on Ru(211) and Pt(211) were 1.3 and 1.4 eV, respectively, whereas a high value of 2.0 eV was found on the Cu(211) surface.[45] As a consequence, $(E_{a,DOH} - E_{a,C=O})$ in eq 5 is assumed to be negative and identical for Ru/m-ZrO_2 and Pt/m-ZrO_2. When $|\Delta H_{GA}|$ is large enough and $(E_{a,DOH} - E_{a,C=O} - \Delta H_{GA}) > 0$, the second term of eq 5 will increase with the reaction temperature and lead to a volcano-type dependence of the r_{C-O}/r_{C-C} ratios on the reaction temperature, as indeed is observed with Ru/m-ZrO_2 (Figure 4). When $|\Delta H_{GA}|$ is small and $(E_{a,DOH} - E_{a,C=O} - \Delta H_{GA}) < 0$, the second term of eq 5 will decrease with the reaction temperature, and thus r_{C-O}/r_{C-C} will decrease with the reaction temperature monotonically, as indeed observed with Pt/m-ZrO_2 (Figure 4). Such analysis suggests that the adsorption of glyceraldehyde on Ru is much stronger than on Pt. Similarly, Abild-Pedersen and Andersson reported that the CO adsorption energy on Ru(0001) and Pt(111) measured at low coverage (0.25 ML) was −1.49 ± 0.22 and −1.37 ± 0.13 eV, respectively, implying a general trend of carbonyl group adsorption on the different noble metal surfaces.[46]

The assumed stronger adsorption of glyceraldehyde on Ru than on Pt accords with the different atmosphere effects of H_2 and N_2 in glycerol hydrogenolysis on 2 wt % Ru/m-ZrO_2 and 2 wt % Pt/m-ZrO_2. As shown in Figure 5, the catalytic activity of Ru/m-ZrO_2 under H_2 was higher than that under N_2, whereas glycerol hydrogenolysis occurred faster under N_2 than H_2 on Pt/m-ZrO_2. To make a rigorous comparison, the initial glycerol hydrogenolysis rates were calculated by extracting the slopes of the fitted conversion profiles at zero reaction time.[18] The initial turnover rates on Ru/m-ZrO_2 under H_2 and N_2 were 0.166 and 0.016 mol glycerol (mol surface Ru·s)$^{-1}$, respectively, showing the much more favorable glycerol reaction under H_2, relative to N_2. For Pt/m-ZrO_2, the reverse order was observed, and the initial rate under H_2 was nearly three times smaller than that under N_2 (0.027 vs 0.072 mol glycerol (mol surface Pt·s)$^{-1}$). The expression of r_{Gly} in eq 1 shows clearly that the presence of H_2 inhibits glycerol hydrogenolysis, provided that the vacant metal sites are readily available, which is consistent with the atmospheric effect of H_2 and N_2 on Pt/m-ZrO_2. The observed opposite effect on Ru/m-ZrO_2 indicates that the concentration of vacant sites on the Ru surfaces play a dominant role in determining the hydrogenolysis turnover rate, most likely because the Ru sites strongly adsorbed glyceraldehyde and other unsaturated intermediates in glycerol hydrogenolysis. Such strong adsorbates are required to be hydrogenated by H_2 to consequently liberate the vacant Ru sites. Thus the glycerol hydrogenolysis rate was much higher under H_2 than that under N_2 on Ru/m-ZrO_2. These results can also account for the observed larger selectivities to the cleavage of C−C bonds and the deep hydrogenolysis to methane on Ru, compared with Rh, Pt, and Pd, which are derived from its stronger adsorption of glyceraldehyde and other unsaturated intermediates in glycerol hydrogenolysis. Mavrikakis and Barteau have pointed out that the adsorption of carbonyl compounds on Group VIII metals is via a η^2(C, O) configuration.[47] Compared with Rh, Pt, and Pd,

dx.doi.org/10.1021/cs400486z | ACS Catal. 2013, 3, 2112−2121

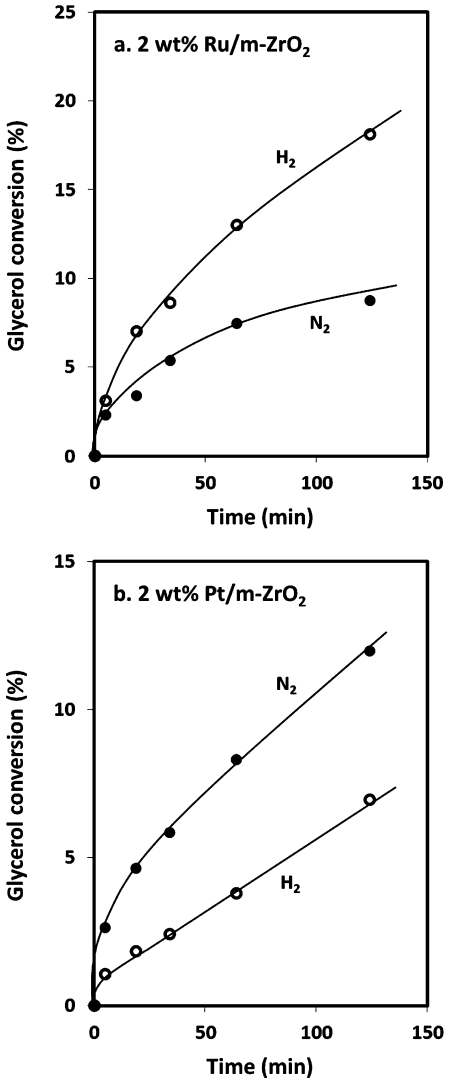

Figure 5. Comparison of glycerol hydrogenolysis rates under H_2 and N_2 on monoclinic zirconia (m-ZrO_2) supported Ru and Pt catalysts with 2 wt % metal loading. (a) 2 wt % Ru/m-ZrO_2; (b) 2 wt % Pt/m-ZrO_2; reaction conditions: 50 cm^3 10 wt % glycerol aqueous solution, 473 K, 6.0 MPa H_2 or N_2, 0.35 g 2 wt % Ru/m-ZrO_2 and 1.0 g 2 wt % Pt/m-ZrO_2 for the reactions under H_2, 2.0 g 2 wt % Ru/m-ZrO_2 and 1.0 g 2 wt % Pt/m-ZrO_2 for the reactions under N_2.

Ru possesses more available unoccupied d orbitals, and thus it can accept more π electrons from the carbonyl intermediates and adsorb them more strongly. This Ru property, according to the Sabatier principle, also leads to its stronger interaction with glycerol to lower the activation barrier of the cleavage of α-C-H bonds during glycerol dehydrogenation to glyceraldehyde, the kinetically relevant step. As a consequence, Ru exhibits a higher catalytic activity than Rh, Pt, and Pd in glycerol hydrogenolysis, as shown in Table 1. Similar effects have been reported for many reactions on the noble metals, for instance, the activity for N_2 dissociation changes in the order of Ru > Rh > Pt, consistent with their d-band unoccupancy.[48]

3.3. Size Effects of Ru Particles on Glycerol Hydrogenolysis. To further understand the activity and selectivity of the Ru catalysts in glycerol hydrogenolysis, we examined the effects of the Ru nanoparticle size. Six Ru/m-ZrO_2 samples were prepared with controllable Ru particle size of diameters in the range of 1.8−4.5 nm by changing the Ru loadings from 0.5 wt % to 5 wt %. The H_2-chemisorption results showed that these samples possessed Ru particle sizes of 1.8, 2.0, 2.3, 3.5, 4.1, and 4.5 nm. As shown in Figure 6, the turnover rate

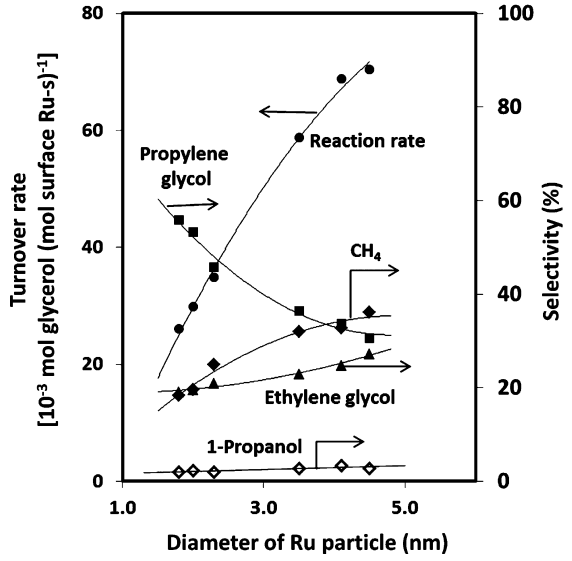

Figure 6. Effects of Ru particle size on turnover rates and selectivities for glycerol hydrogenolysis on monoclinic zirconia supported Ru catalysts. Reaction conditions: 50 cm^3 10 wt % glycerol aqueous solution, 473 K, 6.0 MPa H_2, 3 h, about 20% glycerol conversion obtained by varying the catalyst amount.

(normalized per surface Ru atom) increased by nearly three times monotonically from 0.026 to 0.071 mol glycerol (mol surface Ru·s)$^{-1}$ when increasing the Ru particle size from 1.8 to 4.5 nm at ∼20% glycerol conversion. A similar trend was observed by Montassier et al. in glycerol hydrogenolysis on Ru/C catalysts with Ru particles of diameters in the range of 1.2−4.2 nm.[24] Ru particle size also significantly influenced the product selectivities (Figure 6). At ∼20% glycerol conversion, the increase of the Ru particle size from 1.8 to 4.5 nm led to a decrease of the propylene glycol selectivity from 55.8% to 30.6%, and a concurrent increase of the selectivities to ethylene glycol, 1-propanol, and methane from 19.1% to 27.3%, 1.9% to 2.8%, and 18.3% to 36.1%, respectively. Clearly, the larger Ru particles favor the cleavage of C−C bonds and deep hydrogenolysis reactions, in line with a recent study on the ring-opening of cyclopentane showing that turnover rates of the C−C bond cleavage on Pt/Al_2O_3 increased monotonically with increasing Pt particle size (1−15 nm).[49] Such strong size effects on the catalytic activity and selectivity demonstrate that glycerol hydrogenolysis is a typical structure-sensitive reaction.

It is known that the fraction of edge sites on the surface of metal particles below 5 nm decreases sharply with increase of their particle size while the fraction of terrace sites increases accordingly.[50] The edge sites are more coordinatively unsaturated than the terrace sites. Accordingly, the increase of the Ru particle size weakens the strength of chemisorption of reactants and products on the Ru surface and favors the release of the vacant sites during glycerol hydrogenolysis. Moreover, the weaker interaction between glycerol and the Ru surface leads to the higher activation barrier, that is, the lower kinetic constant, for the cleavage of α-C-H bonds in the kinetically relevant glycerol dehydrogenation step. As shown in eq 1, the turnover rate of glycerol hydrogenolysis is proportional to both the concentration of the vacant metal sites and the kinetic

dx.doi.org/10.1021/cs400486z | ACS Catal. 2013, 3, 2112−2121

constant for the cleavage of the α-C-H bond of glycerol. Therefore, the observed increase in the turnover rate with increasing the Ru particle size is related to the increase in the concentration of the available vacant Ru sites, as a result of the aforementioned weaker adsorption of the reactants and products in glycerol hydrogenolysis.

Rate ratios of the cleavage of the C−O bonds to the C−C bonds reflect the relative activity between the competitive dehydration and decarbonylation reactions of glyceraldehyde, according to eq 5. The selectivity dependence on the Ru particle size in glycerol hydrogenolysis is derived from the site-requirement for cleavage of C−C bonds in the step of glyceraldehyde decarbonylation on the metal surface, considering the dehydration of glyceraldehyde to cleavage of C−O bonds is solely catalyzed by the basic sites on the m-ZrO_2 support, as discussed above. Thus, r_{C-O}/r_{C-C} is determined by $E_{a,C=O}$ and $\Delta S^{\ddagger}_{C=O}$ of glyceraldehyde decarbonylation, ΔH_{GA} and ΔS_{GA} of glyceraldehyde adsorption, and the concentration of the vacant metal sites on the catalyst surface (eq 5). Here ΔS_{GA} and $\Delta S^{\ddagger}_{C=O}$ should change slightly with the Ru particle size because glyceraldehyde and the transition state are both tightly bound to the Ru surface. As discussed above, $|\Delta H_{GA}|$ decreases with the increase of Ru particle size, whereas $E_{a,C=O}$ shows an opposite change. These dual effects will lead to the increase in the second term of eq 5 with increasing Ru particle size. Consequently, the observed higher selectivity to the cleavage of C−C bonds at larger Ru particles in Figure 5 is probably caused by the increase of the available vacant Ru sites, because r_{C-O}/r_{C-C} is inversely dependent on the concentration of the Ru vacant sites, as shown in eq 5. Such analysis suggests that the concentration of the vacant sites on the Ru surface is more critical to r_{C-O}/r_{C-C} than ΔH_{GA} and $E_{a,C=O}$, which is consistent with the fact that C−C bond dissociation usually requires at least two adjacent vacant sites.[51] Taken together, the size effect unveils the determining role of the vacant sites for the catalytic activity and selectivity in glycerol hydrogenolysis on Ru, reflecting the nature of the strong interaction between the Ru particles and oxygenates.[52]

4. CONCLUSIONS

Ru, Rh, Pt, and Pd nanoparticles supported on m-ZrO_2 catalyze glycerol hydrogenolysis to propylene glycol and ethylene glycol, which largely depends on the nature of the metals and their particle size. Their turnover rate decreases in the order of Ru ≫ Rh > Pt > Pd with a similar particle size (∼2 nm), whereas the selectivity ratio of the cleavage of C−O bonds to C−C bonds, leading to propylene glycol and ethylene glycol, respectively, decreases in the reverse order. Both the turnover rate and selectivity to the cleavage of C−C bonds on Ru/m-ZrO_2 increase monotonically with the Ru particle size in the range of 1.8−4.5 nm. Such difference in the rate and selectivity for different noble metals and different particle sizes, based on the analysis of the elementary steps in glycerol hydrogenolysis together with the observed effects of reaction temperature and atmosphere of H_2 and N_2, can be tentatively ascribed to their difference in the adsorption strength of the glycerol and glyceraldehyde intermediate, and so on, as a result of the different availability of their unoccupied d orbitals. These results and their understanding provide directions toward design of more effective metal catalysts for selective hydrogenolysis of glycerol and also other biomass-derived polyols.

■ ASSOCIATED CONTENT

Supporting Information

Derivation details of eqs 1 and 2. This material is available free of charge via the Internet at http://pubs.acs.org.

■ AUTHOR INFORMATION

Corresponding Author

*E-mail: hcliu@pku.edu.cn.

Notes

The authors declare no competing financial interest.

■ ACKNOWLEDGMENTS

This work was supported by National Natural Science Foundation of China (20825310, 21173008, and 51121091) and National Basic Research Project of China (2011CB201400 and 2011CB808700).

■ REFERENCES

(1) Nakagawa, Y.; Tomishige, K. *Catal. Sci. Technol.* **2011**, *1*, 179−190.
(2) ten Dam, J.; Hanefeld, U. *ChemSusChem* **2011**, *4*, 1017−1034.
(3) Ruppert, A. M.; Weinberg, K.; Palkovits, R. *Angew. Chem., Int. Ed.* **2012**, *51*, 2564−2601.
(4) Shen, Y.; Wang, S.; Luo, C.; Liu, H. *Prog. Chem.* **2007**, *19*, 431−436.
(5) Luo, C.; Wang, S.; Liu, H. *Angew. Chem., Int. Ed.* **2007**, *46*, 7636−7639.
(6) Sun, J.; Liu, H. *Green Chem.* **2011**, *13*, 135−142.
(7) Miyazawa, T.; Kusunoki, Y.; Kunimori, K.; Tomishige, K. *J. Catal.* **2006**, *240*, 213−221.
(8) Maris, E. P.; Davis, R. J. *J. Catal.* **2007**, *249*, 328−337.
(9) Feng, J.; Wang, J.; Zhou, Y.; Fu, H.; Chen, H.; Li, J. *Chem. Lett.* **2007**, *36*, 1274−1275.
(10) Li, B.; Wang, J.; Yuan, Y.; Ariga, H.; Takakusagi, S.; Asakura, K. *ACS Catal.* **2011**, *1*, 1521−1528.
(11) Auneau, F.; Michel, C.; Delbecq, F.; Pinel, C.; Sautet, P. *Chem.—Eur. J.* **2011**, *17*, 14288−14299.
(12) Yuan, Z.; Wu, P.; Gao, J.; Lu, X.; Hou, Z.; Zheng, X. *Catal. Lett.* **2009**, *130*, 261−265.
(13) Musolino, M. G.; Scarpino, L. A.; Mauriello, F.; Pietropaolo, R. *Green Chem.* **2009**, *11*, 1511−1513.
(14) Nakagawa, Y.; Ning, X.; Amada, Y.; Tomishige, K. *Appl. Catal., A* **2012**, *433*, 128−134.
(15) van Ryneveld, E.; Mahomed, A. S.; van Heerden, P. S.; Green, M. J.; Friedrich, H. B. *Green Chem.* **2011**, *13*, 1819−1827.
(16) Guo, X.; Li, Y.; Song, W.; Shen, W. *Catal. Lett.* **2011**, *141*, 1458−1463.
(17) Wang, S.; Liu, H. *Catal. Lett.* **2007**, *117*, 62−67.
(18) Wang, S.; Zhang, Y.; Liu, H. *Chem.—Asian J.* **2010**, *5*, 1100−1111.
(19) Wang, S.; Li, Y.; Liu, H. *Acta. Chim. Sinica* **2012**, *70*, 1897−1903.
(20) Huang, Z.; Cui, F.; Kang, H.; Chen, J.; Zhang, X.; Xia, C. *Chem. Mater.* **2008**, *20*, 5090−5099.
(21) Huang, Z.; Cui, F.; Xue, J.; Zuo, J.; Chen, J.; Xia, C. *Catal. Today* **2012**, *183*, 42−51.
(22) Xia, S.; Yuan, Z.; Wang, L.; Chen, P.; Hou, Z. *Appl. Catal., A* **2011**, *403*, 173−182.
(23) Xia, S.; Nie, R.; Lu, X.; Wang, L.; Chen, P.; Hou, Z. *J. Catal.* **2012**, *296*, 1−11.
(24) Zhou, J.; Zhang, J.; Guo, X.; Mao, J.; Zhang, S. *Green Chem.* **2012**, *14*, 156−163.
(25) Maris, E. P.; Ketchie, W. C.; Murayama, M.; Davis, R. J. *J. Catal.* **2007**, *251*, 281−294.
(26) Montassier, C.; Ménézo, J. C.; Hoang, L. C.; Renaud, C.; Barbier, J. *J. Mol. Catal.* **1991**, *70*, 99−110.

(27) Wang, J.; Shen, S.; Li, B.; Lin, H.; Yuan, Y. *Chem. Lett.* **2009**, *38*, 572−573.
(28) Alonso, D. M.; Wettstein, S. G.; Dumesic, J. A. *Chem. Soc. Rev.* **2012**, *41*, 8075−8098.
(29) van Ryneveld, E.; Mahomed, A. S.; van Heerden, P. S.; Friedrich, H. B. *Catal. Lett.* **2011**, *141*, 958−967.
(30) Jiang, T.; Zhou, Y.; Liang, S.; Liu, H.; Han, B. *Green Chem.* **2009**, *11*, 1000−1006.
(31) Musolino, M. G.; Scarpino, L. A.; Mauriello, F.; Pietropaolo, R. *ChemSusChem* **2011**, *4*, 1143−1150.
(32) Miyazawa, T.; Koso, S.; Kunimori, K.; Tomishige, K. *Appl. Catal., A* **2007**, *329*, 30−35.
(33) Alhanash, A.; Kozhevnikova, E. F.; Kozhevnikov, I. V. *Catal. Lett.* **2008**, *120*, 307−311.
(34) Oh, J.; Dash, S.; Lee, H. *Green Chem.* **2011**, *13*, 2004−2007.
(35) Liu, L.; Zhang, Y.; Wang, A.; Zhang, T. *Chin. J. Catal.* **2012**, *33*, 1257−1261.
(36) Li, W.; Huang, H.; Li, H.; Zhang, W.; Liu, H. *Langmuir* **2008**, *24*, 8358−8366.
(37) Choi, M.; Wu, Z.; Iglesia, E. *J. Am. Chem. Soc.* **2010**, *132*, 9129−9137.
(38) Martin, D.; Duprez, D. *J. Phys. Chem.* **1996**, *100*, 9429−9438.
(39) Vasiliadou, E. S.; Heracleous, E.; Vasalos, I. A.; Lemonidou, A. A. *Appl. Catal., B* **2009**, *92*, 90−99.
(40) Deutsch, K. L.; Lahr, D. G.; Shanks, B. H. *Green Chem.* **2012**, *14*, 1635−1642.
(41) Wang, K.; Hawley, M. C.; Furney, T. D. *Ind. Eng. Chem. Res.* **1995**, *34*, 3766−3770.
(42) Roy, D.; Subramaniam, B.; Chaudhari, R. V. *Catal. Today* **2010**, *156*, 31−37.
(43) Ukisu, Y.; Miyadera, T. *React. Kinet. Catal. Lett.* **2004**, *81*, 305−311.
(44) Pham, T. T.; Lobban, L. L.; Resasco, D. E.; Mallinson, R. G. *J. Catal.* **2009**, *266*, 9−14.
(45) (a) Wang, S.; Temel, B.; Shen, J.; Jones, G.; Grabow, L. C.; Studt, F.; Bligaard, T.; Abild-Pedersen, F.; Christensen, C. H.; Nørskov, J. K. *Catal. Lett.* **2011**, *141*, 370−373. (b) *CatApp*; Suncat, SLAC: Menlo Park, CA, 2011; http://suncat.slac.stanford.edu/catapp/.
(46) Abild-Pedersen, F.; Andersson, M. P. *Surf. Sci.* **2007**, *601*, 1747−1753.
(47) Mavrikakis, M.; Barteau, M. A. *J. Mol. Catal. A* **1998**, *131*, 135−147.
(48) Ozaki, A.; Aika, K. Catalytic Activation of Dinitrogen. In *Catalysis: Science and Technology*; Anderson, R. H., Boudart, M., Eds.; Springer Verlag: Berlin, Germany, 1981; Vol. *1*, pp 87−158.
(49) Shi, H.; Gutiérrez, O. Y.; Yang, H.; Browning, N. D.; Haller, G. L.; Lercher, J. A. *ACS Catal.* **2013**, 3, 328−338.
(50) Murzin, D. Y. *J. Catal.* **2010**, *276*, 85−91.
(51) van Santen, R. A. *Acc. Chem. Res.* **2009**, *42*, 57−66.
(52) Peereboom, L.; Jackson, J. E.; Miller, D. J. *Green Chem.* **2009**, *11*, 1979−1986.